Cold Regions Science and Technology 108 (2014) 113–124

Contents lists available at ScienceDirect

Cold Regions Science and Technology

journal homepage: www.elsevier.com/locate/coldregions

# Distributed, explicit modeling of technical snow production for a ski area in the Schladming region (Austrian Alps)

Florian Hanzer [a,b,*], Thomas Marke [a], Ulrich Strasser [a,b]

[a] *Institute of Geography, University of Innsbruck, Austria*
[b] *alpS, Innsbruck, Austria*

ARTICLE INFO

*Article history:*
Received 15 December 2013
Received in revised form 21 July 2014
Accepted 14 August 2014
Available online 21 August 2014

*Keywords:*
Snow modeling
Snowmaking
Snow gun
Technical snow
Artificial snow

ABSTRACT

A module for simulating technical snow production in ski areas coupled to a spatially distributed physically based snow model (AMUNDSEN) is presented. The module explicitly considers individual snow guns and distributes the produced snow along the slopes. The amount of snow produced by each snow gun is a function of the snow gun type, wet-bulb temperature at the snow gun's location, ski area infrastructure (in terms of water supply and pumping capacity), and snow demand. Water losses during snowmaking due to evaporation and sublimation are considered, as well as the distinct properties of technical snow such as the higher density as compared to natural snow. An empirical rule for snow production derived from common snowmaking practices has been implemented, which splits the season into a period of maximum snowmaking and a period of selective on-demand snowmaking. The model is set up for a ski area in the Schladming region (Austrian Alps) using actual snowmaking infrastructure data as model parameters. Model validation is performed for the period 2003–2011 using recordings of snowmaking operations as well as a spatial comparison of remotely sensed and simulated snow-covered area. Simulated total seasonal snowmaking hours and water and energy consumption as well as the ski season length are in good agreement with observations, which indicates that the model is capable of accurately simulating real-world snowmaking operations. The explicit consideration of individual snow guns allows easily playing through different management strategies and changes in snowmaking infrastructure, such as replacing the snow guns with more efficient models, increasing the number of snow guns or concentrating them to certain slope segments, or increasing the capacity of reservoirs.



## 1. Introduction

Winter tourism, most importantly ski tourism, is highly dependent on snow conditions. Natural snow conditions, however, are subject to interannual variability as well as highly sensitive to climate change — rising temperatures lead to less snow precipitation and increased snowmelt, resulting in less reliable snow conditions and a shortening of the ski season. Snowmaking is the main adaptation strategy to these deteriorating natural snow conditions (Scott and McBoyle, 2007), helping to prolong the ski season as well as to guarantee a continuous snow cover during the season. In the Alpine countries, since the installation of the first large-scale snowmaking systems in the mid-1980s, snowmaking has become increasingly important due to the fact that the Alpine region has shown to be particularly affected by climate change — the warming signal since the early 1980s is approximately three-fold amplified as compared to the global trend (Beniston, 2005). Today, almost half of the total skiable terrain in the Alpine countries is equipped with snowmaking systems (Hanzer, 2013), in elevations ranging from valleys as low as 500 m a.s.l. to glaciers (>3000 m a.s.l.) (Mayer et al., 2007). Corresponding numbers from other countries range from 12% in Australia (Pickering and Buckley, 2010) to (varying by region) 50–100% in Canada (Scott et al., 2003) and 66–100% in the United States (Scott and McBoyle, 2007). However, snowmaking operations – besides the need for considerable infrastructural investments in terms of piping, pumps, reservoirs, hydrants, snow guns, compressors, cooling towers, etc. – require large amounts of water and energy and are also dependent on meteorological conditions, as snowmaking is only possible in a certain temperature and humidity range and is increasingly efficient under colder and drier conditions. In Austria, during the extraordinarily warm winter 2006/07 – most likely the warmest European winter for more than 500 years (Luterbacher et al., 2007) – especially low-altitude ski areas could not guarantee continuous skiing operations despite being equipped with snowmaking systems (Steiger, 2011).

Studies investigating the impact of climate change on skiing conditions focusing on natural snow conditions alone project dramatic

* Corresponding author at: Institute of Geography, University of Innsbruck, Austria.
*E-mail address:* florian.hanzer@uibk.ac.at (F. Hanzer).
*URL:* http://www.alpinehydroclimatology.net (F. Hanzer).

http://dx.doi.org/10.1016/j.coldregions.2014.08.003
0165-232X/

decreases in ski season length in the future (e. g., Breiling and Charamza, 1999; Elsasser and Bürki, 2002; Elsasser and Messerli, 2001; Fukushima et al., 2002; Koenig and Abegg, 1997; Moen and Fredman, 2007). Comparatively few studies so far have accounted for the effects of snowmaking when simulating future snow conditions using numerical snow models, which is however necessary in order to obtain more realistic estimates of the future situation. Scott et al. (2003) used a calibrated point-based snow model to calculate future ski season length in southern Ontario (Canada) under current and improved snowmaking conditions, using daily values of air temperature and precipitation in combination with a simple threshold-based snowmaking approach. Other studies applying a similar methodology were performed in Eastern North America (Dawson and Scott, 2012; Scott et al., 2006), Quebec (Scott et al., 2007), and Australia (Hennessy et al., 2003, 2008). Pröbstl and Prutsch (2008) applied a point-based snow model to calculate potential and actual snowmaking hours for selected elevations (valley, intermediate, summit) in an Austrian ski area for current and future climate conditions using daily temperature and precipitation values and a temperature threshold for snowmaking. Steiger and Mayer (2008) calculated potential and required monthly snowmaking days for Tyrolean (Austria) ski resorts in 100 m wide altitudinal bands for current and future temperature conditions using a degree day model and a threshold of −2 °C daily average temperature to define a potential snowmaking day. Steiger (2010) and Schmidt et al. (2012) used an extended version of the original SkiSim model developed by Scott et al. (2003) to estimate future snowmaking potential in Tyrol (Austria) and the Southern Black Forest (Germany), respectively. They introduced a refined snowmaking module and applied the model in a semi-distributed manner in 100 m altitudinal bands. Using daily precipitation as well as minimum, maximum, and mean temperature, they calculated natural snow accumulation, snowmelt, as well as potential snowmaking hours (using a temperature threshold). In a predefined timeframe (the "snowmaking window"), as soon as temperatures are sufficient, snow is produced in all altitudinal bands up to a snow depth of 30 cm. Afterwards, snow is produced in the form of improvement snowmaking, i. e., only when the snow depth falls below a certain threshold value that should be maintained over the course of the season. Olefs et al. (2010) analyzed snowmaking conditions at 14 Austrian stations in various altitudes for the period 1948–2007. They used wet-bulb temperature as a combined measure of temperature and humidity to determine the snowmaking potential at given ambient conditions. Linear regressions between the snow production potential in meters cubed per hour and wet-bulb temperature were derived from technical specifications supplied by four Austrian snow gun manufacturers for both fan guns and lance guns for an average water temperature, water pressure and technical snow density. Hendrikx and Hreinsson (2012) calculated future snowmaking potential for ski areas in New Zealand using a point-based temperature index snow model. Their model incorporated snow gun manufacturer-specified water flow rates to estimate the snowmaking potential using hourly wet-bulb temperatures and produced the maximum possible amount of snow within a given snowmaking window.

All these studies have in common that they were either applied in a point-based or semi-distributed manner, consider snowmaking potential only, or use comparatively simple methods to calculate natural snow depths. To the knowledge of the authors no models currently exist that explicitly quantify technical snow production in a physically based, spatially distributed simulation of the mountain snow cover. In our study, we present a physically based sophisticated snowmaking module incorporated into a fully spatially distributed energy balance snow model (AMUNDSEN, Strasser, 2008). The snowmaking module is capable to distinguish different ski areas in the model domain and explicitly accounts for the technical specifications and locations of individual snow guns. This allows calculating the amount of snow produced by each snow gun (influenced by the type of snow gun, the ambient conditions, and the water supply) and distribute the snow on the slopes, while keeping track of the individual water and power consumption and snowmaking time for each snow gun. We apply the model in an Austrian ski area for historical conditions (2003–2011) in high temporal (hourly time steps) and spatial (10 m grid size) resolution and evaluate the results using snowmaking operation-based recordings provided by the ski area operators.

## 2. Study site and data

### 2.1. Study site

The study site for the present work is a ski area in the Schladming–Dachstein region, in the northwestern part of Styria (Austria). Schladming is located in the Enns valley, an east–west trending valley bordered by the Dachstein Mountains (2995 m a.s.l.) in the north and the Niedere Tauern (max. 2862 m a.s.l.) in the south. Fig. 1 shows the location of the model domain within Austria as well as the individual slopes of the ski area and the meteorological stations surrounding the model domain.

From the ski area operators, comprehensive data sets regarding their infrastructure and operating practices were obtained, providing valuable information for modeling and validation purposes. These data sets include GIS data (ski lifts, slopes, hydrants, pipes, buildings, orthophotos, etc.), locations and types of snow guns, recordings of snowmaking days (snowmaking yes/no) for the seasons 2003/04–2010/11, snow gun-based daily recordings of snowmaking hours as well as water and energy consumption for the seasons 2009/10 and 2010/11, and ski area operating days for the seasons 2003/04–2010/11.

For the present study, the ski area infrastructure of the season 2010/11 was taken as the basis for the simulations. The ski area operates 18 slopes with a total length of approximately 37 km and a total area of approximately 92 ha over an elevation range of 724–1999 m a.s.l. Locations and detailed information on the individual slopes are shown in Fig. 1 and Table 1. As of the season 2010/11, the ski area operates a total of 149 fan guns (no lance guns are in use) of two different manufacturers (in the following named Brand A and Brand B). The 23 Brand B guns (all mobile) are used on the slopes 1, 6, 7, 8, 9, 11, 14, and 15, and the 126 Brand A guns (61 mobile, 58 tower-mounted, 7 mounted on swing arms) on the remaining slopes. Six reservoirs in elevations between 1100 and 1720 m with a total capacity of 235,000 $m^3$ store the water required for snowmaking; additionally, a permanent external water supply from the Enns river with a flow rate of 145 L $s^{-1}$ is available. From a model perspective, accounting for this information allows to simulate technical snow[1] production in unprecedented detail.

### 2.2. The snow model AMUNDSEN

For our study, we applied the modular, physically based, distributed modeling system AMUNDSEN (Strasser, 2008) for the simulation of the natural snow cover and extended it with a new module for the simulation of technical snow production and slope management. AMUNDSEN has been designed to specifically address the requirements of snow modeling in mountain regions under climate change conditions and has been extensively validated in various Alpine sites in the past (Marke et al., 2014 (submitted); Pellicciotti et al., 2005; Strasser, 2004, 2008; Strasser et al., 2008). The functionality of the model includes, among others, several interpolation routines for scattered meteorological measurements (Marke, 2008; Strasser, 2008), rapid computation of topographic parameters from a digital elevation model (Strasser, 2008), simulation of shortwave and longwave radiation including topographic (e.g., shadows) and cloud effects (Corripio, 2003; Greuell et al., 1997), parameterization of snow albedo depending on snow age

[1] Within this paper, we use the term *technical snow* to refer to the snow produced by snow guns, while *artificial snow* refers to the actual snow on the ski slopes, i. e., a compressed and processed mixture of technical snow and natural snow.

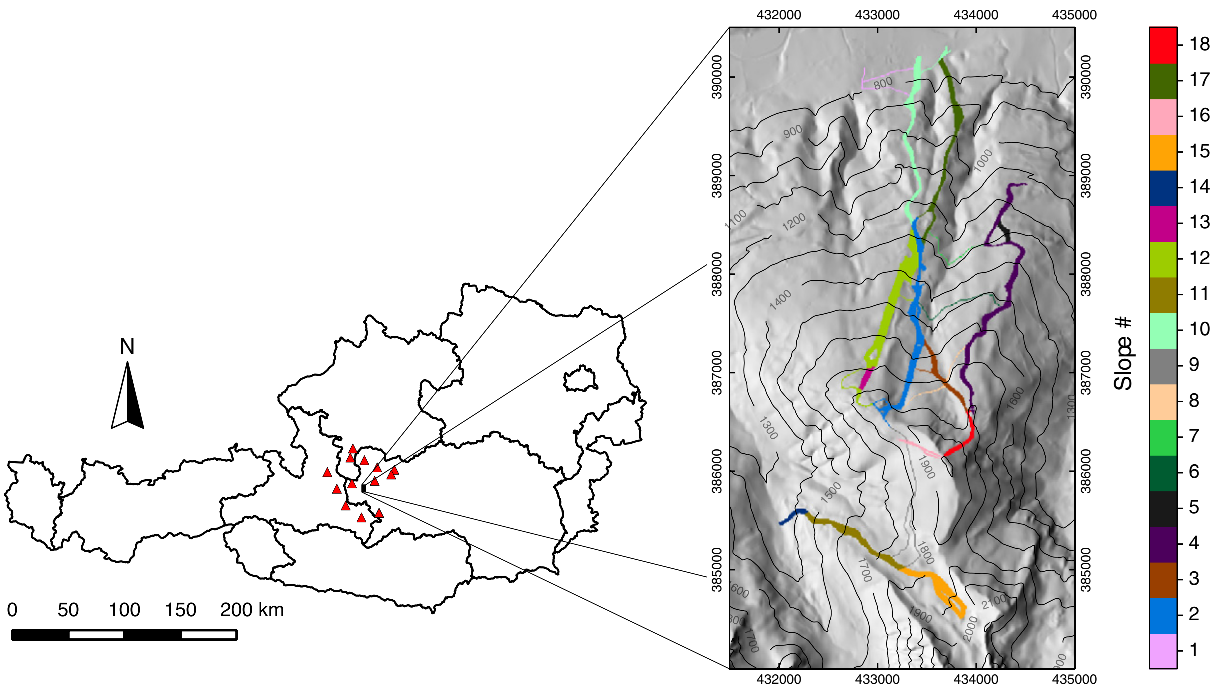


**Fig. 1.** Location of the study region in Austria and the meteorological stations that were used, and map of the model domain showing the individual slopes of the ski area, color-coded with their internally used identifiers. Map coordinates are in meters (coordinate reference system: MGI/Austria Lambert).

and temperature (Rohrer, 1992), parameterization of snow density (Anderson, 1976; Jordan, 1991), and simulation of snowmelt based on an energy balance approach (Strasser et al., 2008). As input data for the simulation of the natural snow cover the model requires a digital terrain model (DTM) of the model domain as well as either hourly, 2-hourly, or 3-hourly recordings of the meteorological variables air temperature, relative humidity, precipitation, global radiation, and wind speed. For the present study, the model was driven with hourly meteorological data and applied on a 10 m × 10 m grid.

For the conversion of simulated snow water equivalent (SWE) to snow depth, it is distinguished between two types of snow layers, herein called new snow and old snow. The density of freshly fallen snow is calculated as a function of air temperature (Anderson, 1976):

$$\rho_{\mathrm{ns}} = \begin{cases} 50 & T_a \leq -15\,^\circ\mathrm{C} \\ 50 + 1.7(T_a + 15)^{1.5} & T_a > -15\,^\circ\mathrm{C}. \end{cases} \tag{1}$$

**Table 1**
List of the slopes in the ski area including their length, area, and elevation range, as well as the number and type of snow guns used as parameters for the snowmaking module in this study.

| Slope | Length [m] | Area [ha] | Min elevation [m] | Max elevation [m] | Number of snow guns | Snow gun type |
|---|---|---|---|---|---|---|
| 1 | 1275 | 1.2 | 746 | 859 | 2 | Brand B |
| 2 | 4259 | 13.2 | 1263 | 1862 | 23 | Brand A |
| 3 | 1646 | 3.9 | 1551 | 1799 | 5 | Brand A |
| 4 | 4863 | 13.4 | 1121 | 1805 | 27 | Brand A |
| 5 | 524 | 1.2 | 1237 | 1325 | 3 | Brand A |
| 6 | 1234 | 0.6 | 1449 | 1527 | 0 | – |
| 7 | 943 | 0.5 | 1266 | 1303 | 0 | – |
| 8 | 1196 | 1.0 | 1647 | 1779 | 2 | Brand B |
| 9 | 1750 | 1.5 | 1725 | 1858 | 2 | Brand B |
| 10 | 3578 | 9.0 | 724 | 1268 | 23 | Brand A |
| 11 | 2028 | 7.0 | 1457 | 1767 | 8 | Brand B |
| 12 | 3899 | 15.8 | 1272 | 1841 | 23 | Brand A |
| 13 | 658 | 1.4 | 1687 | 1783 | 2 | Brand A |
| 14 | 879 | 1.5 | 1329 | 1461 | 3 | Brand B |
| 15 | 1275 | 7.9 | 1759 | 1942 | 6 | Brand B |
| 16 | 1161 | 1.6 | 1825 | 1999 | 2 | Brand A |
| 17 | 3885 | 9.1 | 736 | 1313 | 19 | Brand A |
| 18 | 1520 | 2.4 | 1794 | 1995 | 0 | – |

Snow compaction is calculated for each layer following Anderson (1976) and Jordan (1991), with a phase of rapid compaction for newer snow with densities of less than 150 kg m$^{-3}$, followed by a phase of slower densification which is mainly influenced by the snow load:

$$\frac{\mathrm{d}\rho_s}{\mathrm{d}t} = \rho_s\left(c_1 W^* \mathrm{e}^{-c_2(T^* - T_s)} \mathrm{e}^{-c_3\rho_s}\right), \tag{2}$$

$$\frac{\mathrm{d}\rho_s}{\mathrm{d}t} = \rho_s\left(c_4 \mathrm{e}^{-c_5(T^* - T_s)} c_6\right), \tag{3}$$

$$c_6 = \begin{cases} \mathrm{e}^{-c_7(\rho_s - \rho_d)} & \rho_s > \rho_d \\ 1 & \rho_s \leq \rho_d, \end{cases} \tag{4}$$

with $\rho_s$ [kg m$^{-3}$] being the respective layer's (new snow or old snow) density, $W^*$ [kg m$^{-2}$] the load of snow water equivalent (snow in the layer above and 50% of the snow in the current layer), $c_1 = 0.01$ m$^{-1}$h (new snow), $c_1 = 0.001$ m$^{-1}$h (old snow), $c_2 = 0.08$ °C$^{-1}$, $c_3 = 0.021$ m$^3$kg$^{-1}$, $c_4 = 0.01$ m$^{-1}$h, $c_5 = 0.04$ °C$^{-1}$, $c_7 = 0.046$ m$^3$kg$^{-1}$, $\rho_d = 150$ kgm$^{-3}$ and $T^* = 0$ °C. New snow is converted to old snow when reaching a density of 200 kg m$^{-3}$. The compaction scheme has been calibrated (by slightly adapting the original parameters from Anderson (1976) due to the reduced number of layers in our model) and validated under Alpine conditions using snow depth and SWE measurements. For the present study, an additional *artificial snow* layer was introduced, which is described in more detail in Section 3.6.

### 2.3. Meteorological data

For the present study, corrected station recordings from 13 automatic weather stations (with varying temporal coverage) operated by the Central Institute for Meteorology and Geodynamics (Zentralanstalt für Meteorologie und Geodynamik, ZAMG) surrounding the model domain were used (red triangles in Fig. 1). The stations are located in elevations between 504 m and 1763 m a.s.l.

A meteorological preprocessor in AMUNDSEN is used to spatially interpolate the point information from the station locations to the model domain for every model time step. In case of temperature and precipitation, topographic corrections are carried out by applying monthly temperature lapse rates and elevation adjustment factors, as described by Marke (2008). Humidity is regionalized by first converting from relative humidity to dew point temperature and then applying dew point temperature lapse rates for altitudinal corrections, before a reconversion to relative humidity is carried out (Marke, 2008). The latter is necessary as relative humidity shows a non-linear temperature dependence, while dew point temperature decreases linearly with increasing terrain elevation (Liston and Elder, 2006). Wind speed is corrected for terrain elevation using a linear regression function derived from the station data for a given model time step (Strasser, 2008). Global radiation is spatially distributed by inverting a cloud factor from global radiation at the station locations which is later used to reduce simulated potential direct and diffuse solar radiation separately. For the calculation of global radiation, topographic slope and aspect as well as orographic shadowing and multiple reflection from clouds and surrounding snow covered slopes are taken into account (Strasser, 2008).

Since (especially) solid precipitation in higher altitudes is often considerably underestimated by measurements (e. g., Frei and Schär, 1998; Goodison et al., 1998; Nešpor and Sevruk, 1999), a polynomial elevation-based precipitation correction function was applied for this study. The function has been derived by comparing simulated snow depths and multi-year snow depth measurements at 55 snow gauges in Austria, resulting in an average correction term of approximately 12% per 100 m for solid precipitation. Each pixel of the interpolated precipitation raster is thereby corrected using its elevation $z$ by

$$P_{\text{corr}} = P\left(1 + 3 \times 10^{-7} z^2 - 2.36 \times 10^{-4} z + 6.107 \times 10^{-2}\right). \tag{5}$$

## 3. Methods

### 3.1. Overview and model parameters

An earlier version of the snowmaking module (described in Marke et al., 2014, submitted) was implemented using a pragmatic bulk approach by requiring the total number of snow guns for the ski area as input data and distributing the snow guns evenly across the total slope area. This approach is due to its modest requirements in terms of input data comparatively easily transferable to other ski areas. For the work presented in this study, we implemented an improved version of the snowmaking module which allows for a more detailed simulation of snowmaking operations, however this version also requires comparatively detailed knowledge about the investigated ski area's snowmaking infrastructure. Most importantly, the new module explicitly considers actual snow guns, which are assigned to pixels along the slopes. This has several advantages over the bulk approach — first, for calculating the snow production potential, the ambient conditions (i. e., wet-bulb temperature) at the actual snow gun location (a single pixel) are considered, instead of calculating the snow production potential for the “fractional snow guns” at each slope pixel. This is a more realistic assumption and – in principle – allows replicating the exact real-world snow gun locations in the model. In the current version, however, for each slope only the total number of snow guns needs to be specified, and their respective locations are calculated automatically. Second, snow guns can be turned on or off on demand, and properties such as water flow, snowmaking hours, or energy consumption are tracked individually for each snow gun. The biggest advantage, however, is that different types and behaviors of snow guns can be considered, e. g., each snow gun may have an individual water flow rate, threshold temperature, or power consumption. This also allows easily testing different management strategies, such as replacing lance guns with fan guns, installing higher performance snow guns, or use of snow inducers.

In addition to explicitly considering individual snow guns, several features such as the consideration of limited water availability (reservoir storages) or the calculation of water losses during the snowmaking process have been introduced in the module, which are described in detail in the following sections. Table 2 shows the parameters required by the snowmaking module, while their respective values used in our study (derived from the actual ski area infrastructure) are listed in Tables 1, 3 and 4.

### 3.2. Rules for snowmaking

The decision of when and where to produce snow in a ski area is difficult to describe in a numerical model, as it is influenced by many factors such as ambient conditions, snow demand, economic considerations, and past experiences. Common snowmaking practice is that the snowmaking season is divided into a base-layer snowmaking period before the start of the ski season in order to provide an appropriate ground layer of snow for subsequent natural snowfalls as well as to ensure as early as possible ski season opening (especially before the highly profitable Christmas holidays), and a period of “improvement snowmaking” afterwards, where snowmaking is performed only selectively to maintain a minimum snow depth (Pröbstl, 2006, H. Landl, pers. comm., 2011). At ideal conditions, base-layer snowmaking (corresponding to a minimum snow depth of approximately 30 cm) can be finished in about 50 h with high-end infrastructure (Steiger and Mayer, 2008).

For the present study, the following snowmaking rules were established in accordance with the ski area operators: From November 1 to December 15 the maximum possible amount of snow is produced (only influenced by the ambient conditions and the snowmaking infrastructure). From December 16 to February 28 it is then attempted to maintain a minimum snow base of 60 cm (as suggested by Scott et al., 2007), i. e., snow is only produced when the snow depth is below this threshold.

### 3.3. Placement of the snow guns

As described earlier, the number and type of snow guns has to be specified for each slope. The slopes are subdivided into segments, with each snow gun producing snow exclusively for its respective slope segment. By default, the slopes are divided into segments of equal area, however, using an optional additional parameter snow gun density can be decreased with increasing elevation (i. e., to position more snow guns at lower elevations). Division of the slopes is done by sorting the slope pixels according to their elevation and then iteratively selecting ranges of pixels corresponding to the calculated segment sizes (i. e., we assume that the slopes only go downhill, as is the case for our study area). The snow guns themselves are placed at the pixel corresponding to the median elevation of their respective slope segment.

### 3.4. Modeling of snow production

Generally, two basic methods of snowmaking exist – air-water (lance) guns and fan guns – however, both share the same principle: water is pumped into the snow gun, where it is forced through small nozzles and collides with pressurized air, thus being atomized into small water droplets. These droplets leave the snow gun at high speed and, due to the decompression of the air, freeze into ice crystals before hitting the ground. It is thus crucial to design the snowmaking system in a way that the droplets have ample time to freeze during their way through the atmosphere. The efficiency of snowmaking depends mainly on the ambient conditions, the water temperature, and the nucleation temperature of the water, the latter being able to be increased by use

**Table 2**
Required input data and parameters for the snowmaking module. The columns D (model domain), A (ski area), S (slope), T (snow gun type) indicate for which model element the respective parameter is required.

| Name | Description | Unit/values | D | A | S | T |
|---|---|---|---|---|---|---|
| Ski areas grid | A grid where all pixels belonging to the same ski area are marked with a unique identifier. | 1, 2,... | × | | | |
| Slopes grid | A grid where all pixels belonging to the same slope are marked with a unique identifier. | 1, 2,... | | × | | |
| Maximum water flow | The maximum water flow for the entire ski area (depending on the ski area infrastructure such as pumps, pipes, etc.). | $m^3\ h^{-1}$ | | × | | |
| Capacity of reservoirs | The combined capacity of all reservoirs in the ski area. | $m^3$ | | × | | |
| External water supply | The flow rate of a possible external water supply to refill the reservoirs during the season. | $m^3\ h^{-1}$ | | × | | |
| Number of snow guns | The total number of snow guns on the slope. | ≥0 | | | × | |
| Snow gun type | Type of the snow guns (used for calculating the snow production). | Brand A/B | | | × | |
| Elevation dependency | An optional factor for specifying a possible elevation dependency of the snow gun distribution (e. g., if more snow guns should be placed at lower elevations). | 0…1 | | | × | |
| Threshold wet-bulb temperature | Threshold wet-bulb temperature for which snowmaking is performed. | °C | | | | × |
| Water flow | Water flow as a linear function of wet-bulb temperature. | $m^3\ h^{-1}$ | | | | × |
| Technical snow density | Initial density of the produced snow. | $kg\ m^{-3}$ | | | | × |
| Power consumption | Power consumption of the snow gun (assumed constant). | kW | | | | × |

of snow inducers (additives). Ambient conditions affect the efficiency of heat transfer during the snowmaking process, which occurs by two mechanisms: convective heat transfer and evaporation of water. Radiative heat transfer is insignificant under these conditions (Chen and Kevorkian, 1971; Olefs et al., 2010). Hence, snowmaking efficiency is mainly influenced by air temperature and humidity, which should both be as low as possible. As a combined measure of both temperature and humidity, wet-bulb temperature is commonly used to assess the snowmaking efficiency under given ambient conditions.

Olefs et al. (2010) calculated linear regressions between the snow production potential pp (in cubic meters of snow per hour) and the wet-bulb temperature $T_w$ (in °C) for then present-generation snow guns of four major Austrian snow gun manufacturers. The calculated regression functions are

$$\mathrm{pp}_\mathrm{f} = -4.83T_w + 3.94 \tag{6}$$

for fan guns, and

$$\mathrm{pp}_\mathrm{aw} = -3.94T_w - 4.23 \tag{7}$$

for air–water (lance) guns, and are assumed to be valid for water temperatures of less than 2 °C, a water pressure of 25 bar, wet-bulb temperatures in the range of $-14\ °C \le T_w \le -2\ °C$, and a snow density of 400 $kg\ m^{-3}$.

In our model we adopt this approach by assuming the water flow wf from a snow gun (in cubic meters per hour) to be linearly dependent on the wet-bulb temperature using the general equation

$$\mathrm{wf} = aT_w + b \tag{8}$$

valid for wet-bulb temperatures in the range of $T_{w,\min} \le T_w \le T_{w,\max}$, while allowing to account for different types of snow guns by adapting the parameters $a$, $b$, $T_{w,\min}$, $T_{w,\max}$, as well as the snow density $\rho_\mathrm{ts}$. Table 4 lists the parameters for the different types of snow guns (here referred as Brand A and Brand B) used in this study. For the Brand B guns, the parameters for the regression function (Eq. (8)) were derived from the official product specifications (flow rate as a function of wet-bulb temperature, valid for a water temperature of 1 °C), while for the Brand A guns these specifications were not publicly available, hence we used the parameters for a "generic" fan gun (Eq. (6)) derived by Olefs et al. (2010). Power consumption values are according to the manufacturer's specifications for both snow gun types.

Wet-bulb temperature is calculated in the model by numerically solving the psychrometric equation

$$\Delta e = e_l - (e_w - \gamma(T_a - T_w)) \tag{9}$$

for $\Delta e = 0$. Here,

$$e_l = \frac{\mathrm{RH}}{100} e_s \tag{10}$$

is the water vapor partial pressure in hPa, RH the relative humidity in percent,

$$e_s = \begin{cases} 6.1078 \exp\left(\dfrac{17.08085T_a}{234.175 + T_a}\right) & T_a \ge 0\ °\mathrm{C} \\ 6.1071 \exp\left(\dfrac{22.4429T_a}{272.44 + T_a}\right) & T_a < 0\ °\mathrm{C} \end{cases} \tag{11}$$

the saturated vapor pressure at ambient temperature in hPa, and $e_w$ the saturated vapor pressure for the wet-bulb temperature (calculated by evaluating Eq. (11) with $T_w$ instead of $T_a$).

$$\gamma = C_p \frac{p}{L_v} \tag{12}$$

is the psychrometric constant in hPa $K^{-1}$,

$$L_v = 2.5014 \times 10^6 - 2361T_a \tag{13}$$

the latent heat of vaporization in J $kg^{-1}$, and

$$C_p = C_{p,\mathrm{dry}}(1 + 0.84\ \mathrm{SH}) \tag{14}$$

the specific heat capacity of moist air in J $kg^{-1}$ $K^{-1}$, with $C_{p,\mathrm{dry}} = 1004.67$ J $kg^{-1}$ $K^{-1}$ the specific heat capacity of dry air, and

$$\mathrm{SH} = \frac{0.622e_l}{p - 0.378e_l} \tag{15}$$

**Table 3**
Ski area parameters used for the study.

| | |
|---|---|
| Maximum water flow [$m^3\ h^{-1}$] | 2481 |
| Reservoir capacity [$m^3$] | 195,000 |
| External water supply rate [$m^3\ h^{-1}$] | 522 |
| External water supply capacity [$m^3$] | Unlimited |

**Table 4**
Model parameters for the snow guns used in this study.

| Type | $a$ | $b$ | $T_{w,\min}$ | $T_{w,\max}$ | $\rho_\mathrm{ts}$ | $P$ |
|---|---|---|---|---|---|---|
| | [$m^3\ h^{-1}\ °C^{-1}$] | [$m^3\ h^{-1}$] | [°C] | [°C] | [$kg\ m^{-3}$] | [kW] |
| Brand A | −1.93 | 1.58 | −14 | −2 | 400 | 23.5 |
| Brand B | −1.46 | 3.33 | −14 | −3 | 400 | 27.0 |

the specific humidity. Atmospheric pressure $p$ (in hPa) is calculated by assuming a linear temperature gradient in the free atmosphere:

$$p = 1013.25\left(1 - \frac{g_a h_e}{280}\right)^{\frac{M_a g}{R g_a}}, \tag{16}$$

where

$$g_a = \begin{cases} -0.0098\,\mathrm{K\,m^{-1}} & (\text{no rain}) \\ -0.0065\,\mathrm{K\,m^{-1}} & (\text{rain}) \end{cases} \tag{17}$$

is the atmospheric temperature gradient, $h_e$ the elevation above sea level, $M_a = 28.97$ g mol$^{-1}$ the molecular mass of dry air, $g = 9.81$ m s$^{-2}$ the Earth-surface gravitational acceleration, and $R = 8.314$ J mol$^{-1}$ K$^{-1}$ the universal gas constant.

Eq. (8) describes the maximum water flow for a snow gun under given meteorological conditions. The actual water consumption for all snow guns in a given time step is calculated as follows:

- First, depending on the date and the meteorological and/or snow conditions (see Section 3.2), it is decided which snow guns are activated (all, or only those which need to maintain a 60 cm snow base).
- Then, the possible water flow for all active snow guns is calculated using Eq. (8) and added up to derive the possible total water flow for the entire ski area $\mathrm{wf_{tot}}$ (without yet considering infrastructural limitations). The corresponding possible total water consumption for the ski area $\mathrm{wc_{tot}}$ can then be expressed as

  $$\mathrm{wc_{tot}} = \mathrm{wf_{tot}} \cdot \Delta t, \tag{18}$$

  with $\Delta t$ as the time step duration in hours.
- The actual total water consumption $\mathrm{wc_{act}}$ is limited by the maximum water flow $\mathrm{wf_{max}}$ and the amount of water stored in the reservoirs ws:

  $$\mathrm{wc_{act}} = \min\{\mathrm{wc_{tot}}, \mathrm{wf_{max}} \cdot \Delta t, \mathrm{ws}\}. \tag{19}$$

- The snowmaking time (i.e., the duration for which the snow guns are active in the current time step) in hours for each active snow gun is then

  $$\mathrm{st} = \frac{\mathrm{wc_{act}}}{\mathrm{wc_{tot}}} \cdot \Delta t, \tag{20}$$

  and the water and energy consumption (in m$^3$ and kW h, respectively) accordingly

  $$\mathrm{wc} = \mathrm{wf} \cdot \mathrm{st}, \tag{21}$$

  $$\mathrm{ec} = P \cdot \mathrm{st}. \tag{22}$$

### 3.5. Water losses during snowmaking

Water losses during snowmaking (i. e., during the time the water droplets are airborne) due to evaporation and sublimation are calculated following the approach of Eisel et al. (1988), who derived an energy balance model for the snowmaking process. The water vapor loss $m_v$ (in kg h$^{-1}$) at ambient temperature for each snow gun can be expressed as

$$m_v = 1000\,\mathrm{wf}\,\frac{e_s}{e_{s,0}}\,\frac{c_i + T_{water} c_{sw}}{c_i + L_{v,0}}, \tag{23}$$

with 1000wf as the water flow in kg h$^{-1}$, $T_{\mathrm{water}}$ as the water temperature in °C, $c_{\mathrm{sw}} = 4.18 \times 10^3$ J kg$^{-1}$ K$^{-1}$ as the specific heat of water, $c_i = 3.375 \times 10^5$ J kg$^{-1}$ as the melting heat of ice, $L_{v,0} = 2.5014 \times 10^6$ J kg$^{-1}$ as the latent heat of vaporization at 0 °C, and $e_{s,0} = 6.11$ hPa as the saturated vapor pressure at 0 °C.

For typical snowmaking conditions (air temperatures between −20 and 0 °C and water temperatures between 1 and 5 °C), the resulting water losses are in the range of 2–13%, which is in agreement with the ranges given by Olefs et al. (2010), who estimated the losses to be around 5–15% for fan guns and 15–40% for lance guns (these values, however, also include losses due to wind drift, which we do not consider in our calculations). As the water temperature has a comparatively small effect on the resulting water losses, for our calculations a constant water temperature of 1 °C was assumed.

### 3.6. Snow on the slopes

When a snow gun is active, its water consumption is calculated according to Eqs. (8) and (21). Aside from the water vapor losses during the snowmaking process due to evaporation and sublimation, which are calculated according to Eq. (23), we assume that the entire water is converted to snow using the respective snow gun's snow density $\rho_{\mathrm{ts}}$, i.e., there is no liquid water remaining. As we also do not consider wind drift losses, the entire snow produced by the snow gun is distributed evenly among its target pixels. To account for the distinct properties of the machine-made snow, a new *artificial snow* layer type has been introduced in AMUNDSEN, whose properties are as follows:

- The water equivalent of the produced technical snow is distributed equally among the snow gun's target pixels at the artificial snow layer.
- The artificial snow layer incorporates the new snow and old snow layers, i.e., as soon as technical snow is produced, possibly existing new snow and old snow layers along with their properties are merged into the new artificial snow layer at the respective pixels (the water equivalent of the new snow and old snow layers is added to the artificial snow layer's water equivalent, while for density and albedo a weighted mean of the three layers is calculated).
- The initial density of technical snow $\rho_{\mathrm{ts}}$ is assumed according to Table 4. For the densification according to Eqs. (2) to (4), artificial snow is assigned the same parameters as new snow; with the exception of the parameter $c_1$ of Eq. (2), which is enlarged to a value of 0.5 m$^{-1}$ h each day at midnight in order to implicitly account for the increased snow compaction due to slope grooming.
- Following Keller et al. (2004), a more rapid albedo decline is assumed for artificial snow. Since no measurements of albedo on the ski slopes were available or could be found in the literature, we assume the albedo decline to be twice as fast as for natural snow.

In AMUNDSEN, snow accumulation is calculated as the sum of natural and technically produced snow, with snowmelt determined by the energy surplus at the snow surface.

### 3.7. Ski season length

Most studies define ski season length as the number of days with a snow depth of at least 30 cm in a certain period (e. g., Hendrikx and Hreinsson, 2012; Koenig and Abegg, 1997; Moen and Fredman, 2007; Rixen et al., 2011; Schmidt et al., 2012; Scott et al., 2003, 2006, 2007). We use a similar approach, however assume that skiing operations continue even if the snow depth falls below this threshold during the season, as long as a minimum snow base of 20 cm is maintained:

- Starting from November 1, as soon as the snowpack is at least 30 cm thick over five consecutive days, the *ski opening date* is set to the first of those five days.
- Starting from the ski opening date, as soon as the snowpack is less than 20 cm thick over ten consecutive days, the *ski closing date* is set to the first of those ten days. In accordance with common management practices for Austrian ski areas, we additionally limit the latest closing date to the Sunday after Easter or April 15 (to prevent too early closing), whichever is later.

- The ski season length is calculated as the number of days between the opening and the closing date, i.e., it is assumed that the ski area does not close during the season.

On the basis of these assumptions, a season length can be calculated for every pixel of the model domain. To estimate the season length on a ski area basis, first the season length for each slope is calculated as the number of days between the latest opening date and the earliest closing date of all slope pixels. The ski area season length is then selected as the maximum season length of all individual slopes.

## 4. Results

In the following, we describe the results of the model simulations for the period 2003–2011. The simulations were performed with the parameters for the snowmaking module as listed in Tables 1, 3 and 4. Fig. 2 shows the resulting locations of the snow guns as assigned by the model.

Again, it has to be noted that all simulations have been performed on the basis of the 2010/11 snowmaking infrastructure, since for earlier seasons the required detailed information regarding snow gun types and locations was unavailable. The snowmaking infrastructure in the ski area has been completely renewed and considerably extended during the period 2006–2010. This includes exchanging almost all existing snow guns with more efficient models and considerably increasing the total number of snow guns, installing new reservoirs (increasing the capacity from 125,000 to 195,000 $m^3$), increasing the external water supply rate (from 60 to 145 L $s^{-1}$) as well as renewing the piping and pumping system. Hence, only the model results of the season 2010/11 are directly comparable to observational data, while for earlier seasons the model is expected to overestimate technical snow production.

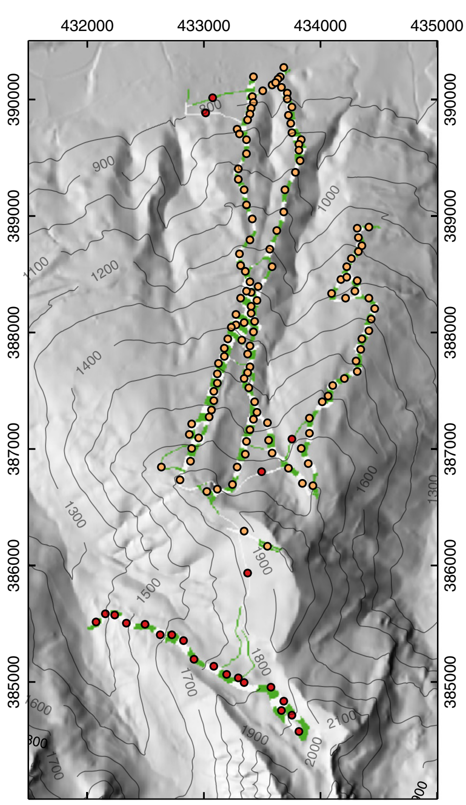


**Fig. 2.** Locations of the snow guns (orange: Brand A, red: Brand B) and the associated slope segments as assigned by the model.

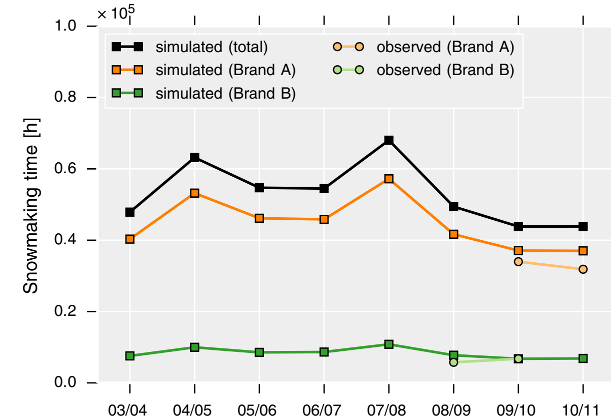


**Fig. 3.** Simulated and (where available) observed total seasonal snowmaking time for the seasons 2003/04–2010/11.

### 4.1. Snowmaking time

Fig. 3 shows the total seasonal modeled and (where available) observed snowmaking time for the seasons 2003/04–2010/11. In the seasons with observational data, the total snowmaking hours for the Brand A snow guns are overestimated by 9% in 2009/10 and by 16% in 2010/11, while for the Brand B guns, they are overestimated by 34% in 2008/09 and within 0.1% of the observations in 2009/10.

Fig. 4 shows the observed and modeled daily snowmaking time per snow gun (Brand A snow guns only) for the seasons 2009/10

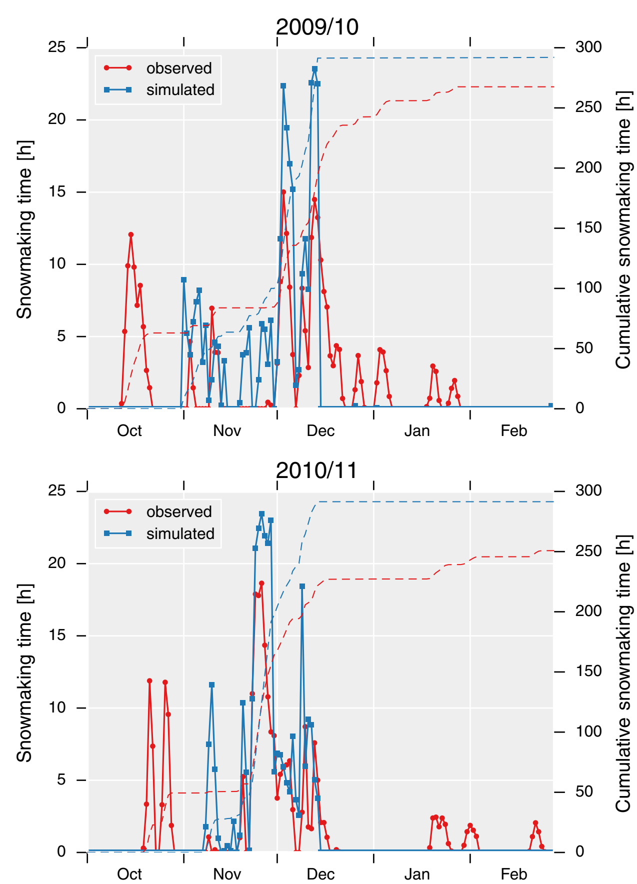


**Fig. 4.** Observed and simulated daily snowmaking time (averaged over number of snow guns) for the seasons 2009/10 and 2010/11 (Brand A snow guns only; cumulative results displayed as dashed lines).

and 2010/11. The observations reveal that, if the ambient conditions allow it, first snowmaking is already done in mid-October, while the model assumes snowmaking to start at the earliest on November 1. During the base-layer snowmaking period from November 1 to December 15, the observed snowmaking days (snowmaking yes/no) are very well reproduced for the season 2010/11, with only two short periods in mid-November and early December, where snow was produced in the model while not in reality. This is also the case for most of November in the season 2009/10, while for the first half of December the snowmaking days are again reproduced well. The actual amounts of snowmaking hours, however, tend to be largely overestimated, especially during the season 2009/10. This is on the one hand probably due to the larger number of snow guns in the model as compared to reality in this season, but also due to the fact that snowmaking in the model always starts at $T_w = -2$ °C for Brand A guns (see Table 4), while in reality the snowmakers might apply lower threshold temperatures, depending on the current snow demand and their experience. In both displayed seasons, snow depth on the slopes (almost) never falls below 60 cm until the end of February, hence only negligible amounts of snow are produced after the end of the base-layer snowmaking period. In reality however, considerable amounts of additional snow (10–15% of the total seasonal snow production in these two seasons) are produced during periods with optimal snowmaking conditions in January and February.

Fig. 5a shows for the season 2010/11 the spatially distributed total seasonal snowmaking time (i.e., for each slope pixel, the time for which its corresponding snow gun has been active). Since in this season snowmaking was mainly performed during the maximum snowmaking period (see Fig. 4), snowmaking time is mainly dependent on elevation (corresponding to wet-bulb temperature conditions) in this case.

For the seasons 2003/04–2008/09, only recordings of snowmaking days (snowmaking yes/no) are available. Fig. 6 shows the observed and simulated monthly snowmaking days for the seasons

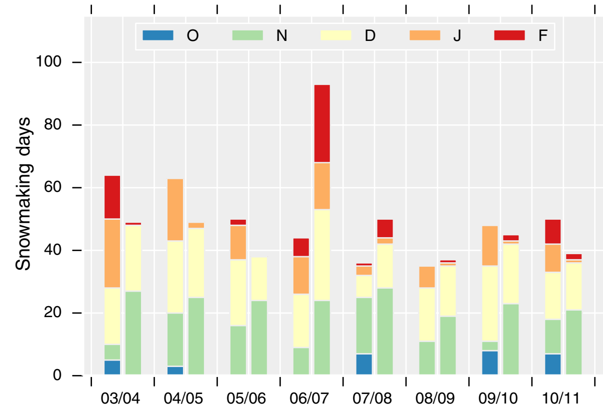


**Fig. 6.** Monthly snowmaking days for the seasons 2003/04–2010/11. The two bars for each season depict the observed (first bar) and simulated (second bar) snowmaking days (for the model results, only days with a total snowmaking time of at least 5 h were counted).

2003/04–2010/11. To account for the local snowmaking practice, for the model results only days with a total snowmaking time of at least 5 h were counted. Simulated snowmaking days are within ± 15 d of the observations for all seasons except the exceptionally warm winter 2006/07 (with the mean winter temperature in the study region being approximately 3 °C above average), where the model simulates more than double the number of snowmaking days as compared to the observations. Further investigations reveal that for most parts of this season, snowmaking conditions are extremely unfavorable, however snowmaking is still possible (wet-bulb temperatures below the threshold). Hence, during the maximum snowmaking period (November to mid-December), snow is produced every day when the conditions allow it, although

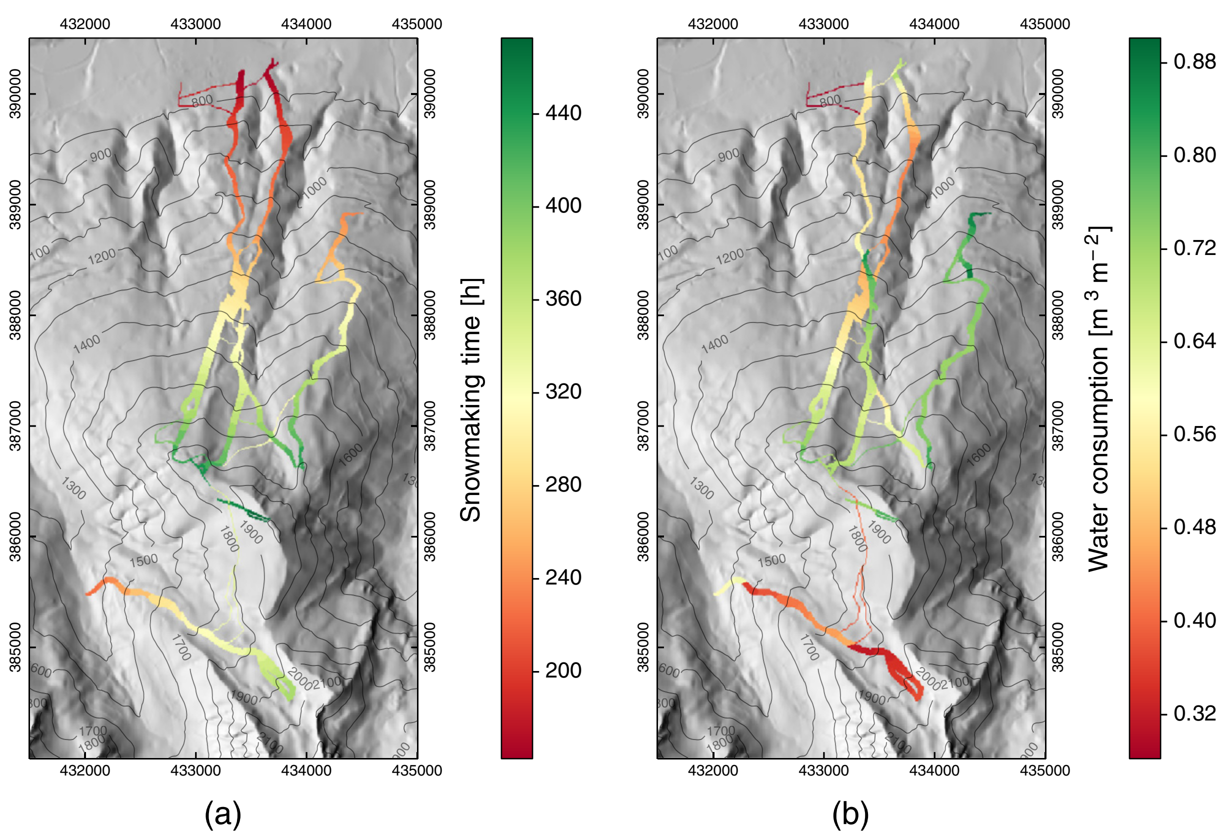


**Fig. 5.** Spatially distributed seasonal snowmaking time (a), and water consumption (b) for the season 2010/11.

only for shorter durations and less efficiently (due to the decreased water throughput). Due to the higher temperatures (less natural snowfall and increased melt), snow depths on the slopes frequently fall below the 60 cm threshold, hence in this season also in the "improvement snowmaking" period from mid-December to February snow is produced almost every day when the conditions allow it. In reality, the base-layer snowmaking was performed in this season during a few days in early and mid-November with favorable snowmaking conditions, while afterwards maximum possible amounts of snow were produced during cold periods, which allowed snowmaking to be stopped during periods with unfavorable conditions.

### 4.2. Water consumption

Fig. 7 shows the total seasonal modeled and (where available) observed water consumption for the seasons 2003/04–2010/11. For the seasons with observational data (Brand A guns), the simulated water consumption is underestimated by approximately 15% in the season 2009/10, while it is within 0.5% of the observations in the season 2010/11. This underestimation of water consumption in combination with the overestimation of snowmaking hours in both seasons suggests that a certain portion of technically produced snow can be attributed to times with unfavorable snowmaking conditions, resulting in inefficient snow production.

Fig. 8 shows the observed and simulated daily water consumption per snow gun (Brand A snow guns only) for the seasons 2009/10 and 2010/11. The curves are similar to the daily snowmaking hours, although of course water consumption is additionally influenced by the ambient conditions. In the season 2010/11, the influence of water availability on snowmaking can be seen: Starting from late November, the reservoirs are empty and (despite favorable snowmaking conditions) the water flow is limited to the external supply rate (see Table 3). For two days (December 7–8), snowmaking conditions then deteriorate while the reservoirs continue to be refilled, resulting in a peak in water consumption on the next day as soon as snowmaking is continued, followed again by a period of limited water availability.

### 4.3. Energy consumption

Fig. 9 shows the observed and simulated daily energy consumption per snow gun (Brand A snow guns only) for the seasons 2009/10 and 2010/11. As for the snow guns a constant power consumption is assumed (depending on the snow gun type, see Table 4), the curves generally show the same course as the snowmaking hours.

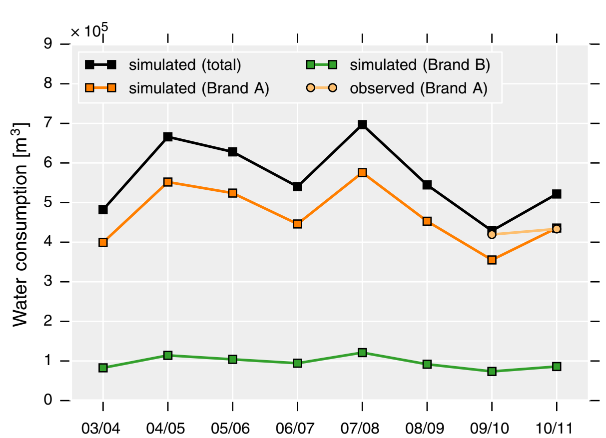


**Fig. 7.** Simulated and (where available) observed total seasonal water consumption for the seasons 2003/04–2010/11.

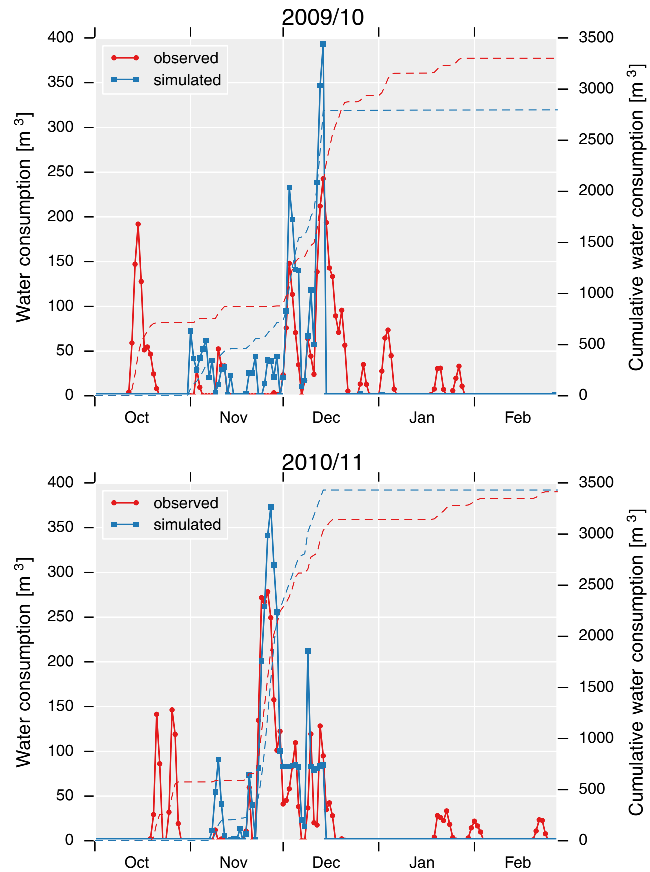


**Fig. 8.** Observed and simulated daily water consumption (averaged over number of snow guns) for the seasons 2009/10 and 2010/11 (Brand A snow guns only; cumulative results displayed as dashed lines).

### 4.4. Ski season length

Fig. 10 shows the actual (observed) ski season length for the seasons 2003/04–2010/11 as well as the simulated season length (with and without snowmaking) according to the rules described in Section 3.7. Deviations from the observed and simulated season length (with snowmaking) are less than one week for the four seasons 2007/08–2010/11, while the season length is overestimated by 3–4 weeks for the seasons further in the past. This is not surprising however, since the model runs were performed using the snowmaking infrastructure data for the season 2010/11 and not the actual data of the respective years. Starting with the season 2006/07, the snowmaking infrastructure in the ski area was considerably extended, which is a possible explanation for the increased season lengths (and better agreement with the model results) afterwards. The simulated season length for natural snow conditions only (dashed line in Fig. 10) shows considerable interannual variations as well as is – for most seasons – significantly shorter than the season length with snowmaking considered. In the season 2006/07, according to the simulations skiing would not have been possible at all without snowmaking.

### 4.5. Spatial validation

For selected dates between mid-April and late May (i.e., around or after the end of the ski season) with available remote sensing observations (Landsat 7 ETM + scenes), Table 5 shows the fractional snow-covered area (SCA) of the slope pixels for the observations and the simulations, as well as the pixel-based agreement between

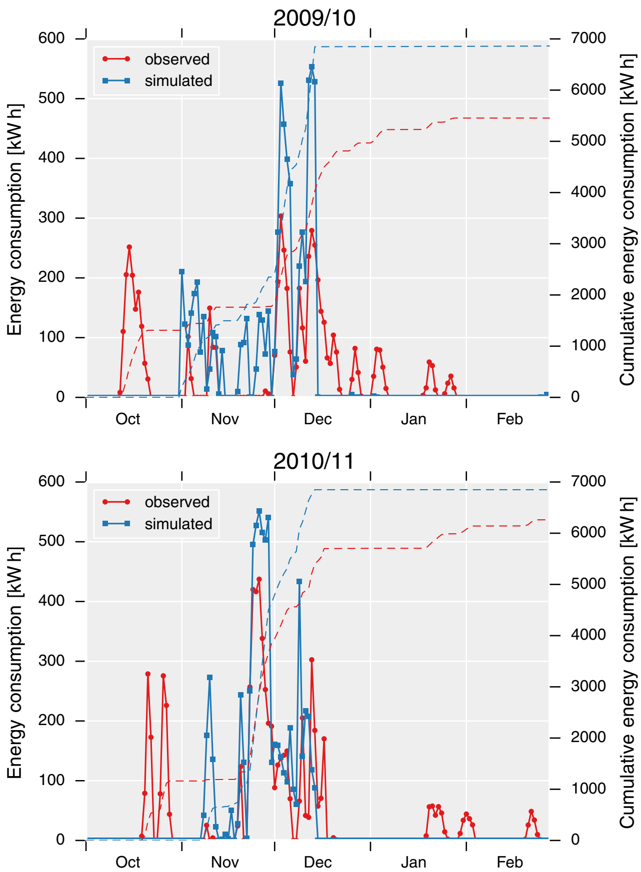


**Fig. 9.** Observed and simulated daily energy consumption (averaged over number of snow guns) for the seasons 2009/10 and 2010/11 (Brand A snow guns only; cumulative results displayed as dashed lines).

observations and model results (i.e., the fraction of pixels correctly classified by the model). The Landsat images were classified by calculating the normalized difference snow index (NDSI) (Hall et al., 1995) and applying a threshold value of 0.4 (Dozier and Painter, 2004), while the model results were classified as snow-covered for SWE values ≥1 mm. Fig. 11 shows the simulated SWE for April 9, 2011 and the corresponding Landsat image. The results indicate that in the model generally parts of the slopes become snow-free too early, as shown by the lower SCA values (with one exception), which seems unexpected, since the (extended) snowmaking infrastructure is applied also for seasons in the past, and the season length is being

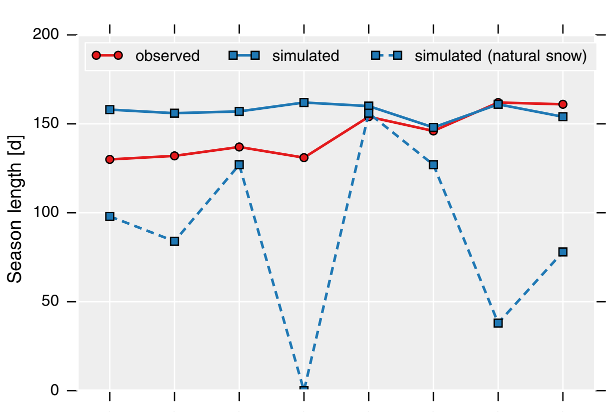


**Fig. 10.** Observed and simulated (with (solid line) and without (dashed line) snowmaking) ski season length for the seasons 2003/04–2010/11.

**Table 5**
Observed and simulated fractional snow-covered area (SCA) of the slope pixels and agreement (i.e., fraction of pixels correctly classified by the model) for selected dates in April and May. Observed SCA is derived from Landsat 7 ETM+ scenes using an NDSI threshold of 0.4, and simulated SCA is derived using an SWE threshold of 1 mm.

| Date | SCA observed | SCA simulated | Agreement |
|---|---|---|---|
| 2005-04-15 | 0.864 | 0.978 | 0.872 |
| 2007-04-14 | 0.712 | 0.482 | 0.714 |
| 2007-04-21 | 0.507 | 0.258 | 0.668 |
| 2010-04-22 | 0.876 | 0.545 | 0.658 |
| 2010-04-29 | 0.736 | 0.271 | 0.526 |
| 2010-05-24 | 0.282 | 0.005 | 0.722 |
| 2011-04-09 | 0.764 | 0.767 | 0.794 |

overestimated for those seasons (Fig. 10). Possible explanations for this result could be that in the model too much snow is produced at higher elevations (hence the season length overestimation) and not enough at lower elevations (hence the lower SCA values) due to an overrepresentation of snow guns in higher elevations (which could be compensated by adapting the elevation dependency factor (see Table 2) for the respective slopes), natural snow amounts are underestimated, or snowmelt is overestimated (possibly due to an underestimation of the artificial snow albedo).

## 5. Discussion and conclusions

In our study, a spatially distributed snowmaking module has been incorporated into a physically based energy balance snow model, and applied and evaluated for a ski area in Austria. The snowmaking module explicitly considers individual snow guns and the meteorological conditions at their locations, calculates water losses during the snowmaking process due to evaporation and sublimation, and accounts for the available water supply and pumping capacity in the ski area, making it to our knowledge the most detailed approach for the modeling of snowmaking operation so far. However, the model requires comparatively high temporal (hourly to three-hourly) as well as spatial (depending on the ski area max. 10–50 m, since it is necessary that the area of the rasterized slopes matches the real slope area most closely in order to generate realistic snow depths) input data resolutions, leading to high computational costs. In addition, in order to accurately simulate snowmaking operations, detailed specifications about the ski area infrastructure (pumping capacity, water supply, number of snow guns) and snow guns (wet-bulb temperature-dependent water flow) as well as snowmaking operations (snowmaking window, threshold temperatures, minimum snow depth that should be maintained) should be available.

Our results show that for the few seasons for which observational data are available, the model performs well in terms of reproducing the total seasonal snowmaking time, water consumption, and energy consumption. For the comparisons on a daily basis, only for the peak snowmaking period (early to mid-December in 2009/10, and mid-November to mid-December in 2010/11) daily snowmaking amounts are reproduced well. This effect can be traced to the general assumptions made on the snowmaking periods, which might differ from the individual decisions made by the snowmaking experts in the ski area. In reality, in the two examined seasons considerable snow amounts in the form of depot snow are already produced during cold periods in October, while only little snow amounts are then produced during periods with more unfavorable snowmaking conditions in November. In the current model version, snowmaking starts at the earliest in November, where as soon as the temperatures are below the threshold snow is produced immediately and for up to 24 h a day, while in reality even with fully automated modern snowmaking systems snowmaking operations always depend on local practices and experiences from previous seasons. This becomes especially apparent in the “improvement snowmaking” period, where in the

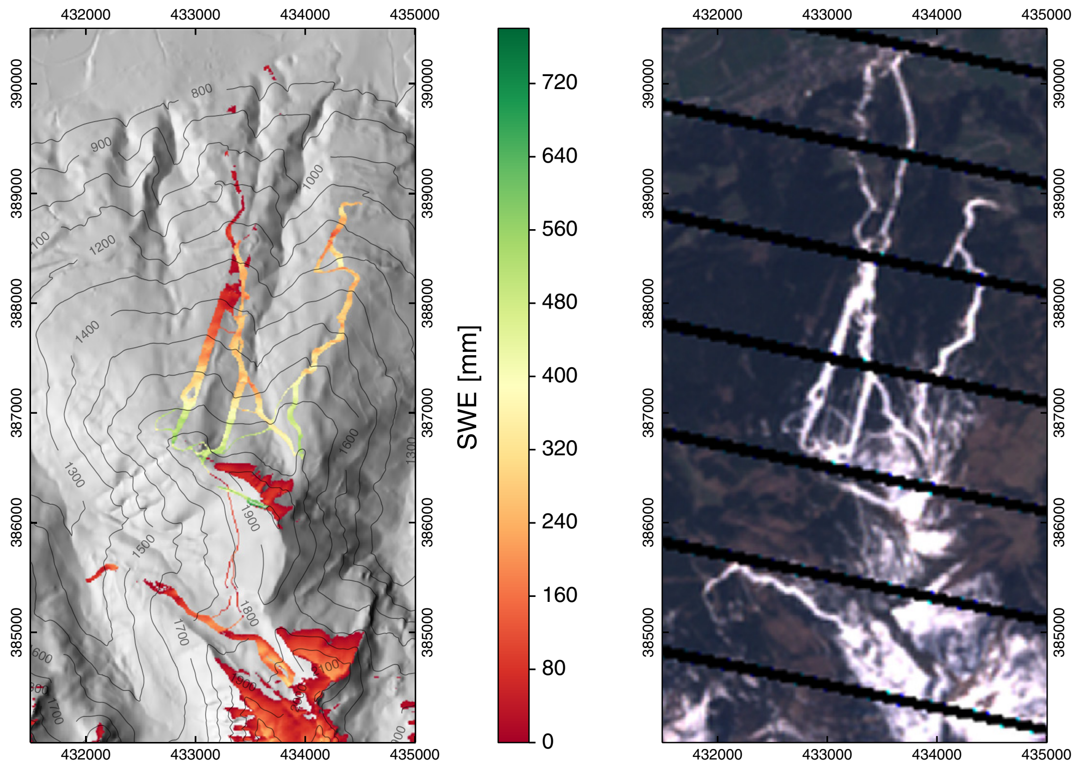


**Fig. 11.** Simulated SWE for April 9, 2011 (snow-free pixels are transparent) and the corresponding Landsat 7 ETM+ scene (RGB image).

model snowmaking is performed continually as long as the snow depths are below 60 cm (and only until they are exactly 60 cm), while in reality only during periods with favorable snowmaking conditions larger amounts of additional snow are produced. For a more accurate simulation of these processes, the snowmaking rules in the model could be refined in accordance with local practices, however, the currently implemented rule set should cover general practices applicable for most Austrian or Alpine ski areas.

The lack of a blowing snow module in the model setup may represent a limitation of this study. Snow transport by wind is a major factor in determining the heterogeneous snow distribution in complex terrain, generally resulting in erosion of snow in exposed areas (e.g., windward slopes or convex areas) and deposition of snow in sheltered areas (e.g., leeward slopes or small-scale depressions) — snow depths in sheltered areas can be several times as high than on adjacent exposed areas (Dadic et al., 2010; Föhn and Meister, 1983; Schirmer et al., 2011). With regard to our study area, we have estimated the significance of the following possible types of blowing snow events: i) Large-scale topography-induced redistribution events likely do not play a major role in our study region, due to the comparatively low elevation and gentle topography of the terrain. Significant redistribution events are expected to occur only near the exposed ridges at the highest elevated parts of the ski area. Additionally, most ski slopes are in forested areas, where wind speeds are lower than in open terrain. ii) Erosion of snow from the ski slopes is very limited due to the high degree of cohesive bonding between the snow crystals, resulting from the accelerated sintering of technical snow as compared to natural new snow as well as the additional hardening due to mechanical processing (Fauve et al., 2002). iii) Snow might be transported to the ski slopes from the surrounding forest canopy, however this effect depends on several factors such as the size of the openings and their orientation relative to the wind direction (Schmidt and Troendle, 1989; Varhola et al., 2010). Due to the lack of measurements for our study area or numerical models that are able to simulate this effect, we are unfortunately unable to estimate if it leads to any significant snow gains on the slopes. iv) Blowing snow during the production of technical snow is again likely insignificant due to the use of low-mounted fan guns and the low wind speeds in forested areas. However, simulating and quantifying all these effects would require substantial effort and was beyond the scope of the present work.

In this study we have focused on evaluating the model's ability to reproduce the historical conditions when driven with the current (as of the season 2010/11) infrastructural conditions as input data. However, the main advantage of this advanced snowmaking simulation approach as compared to simpler methods is the possibility to easily play through different management options and changes in snowmaking infrastructure. For example, one could examine the effects of upgrading the snowmaking infrastructure in terms of pumping capacity and reservoirs, increasing the number of snow guns, concentrating the snow guns to certain altitudes or slope segments, replacing lance guns with fan guns, installing higher performance snow guns (increased water flow and/or higher threshold temperatures), or use of snow inducers. Testing these management options including their analysis of economic effects is envisaged in future research projects.

## Acknowledgments

We would like to thank the investigated ski area for providing extensive ski area and snowmaking operations related data, as well as the Austrian Central Institute for Meteorology and Geodynamics (ZAMG) for providing meteorological data. Special thanks go to Robert Steiger for supporting the development of the snow production approach with his expert knowledge on the snowmaking practice in Austrian ski areas. We also thank the two anonymous reviewers who helped to improve the paper considerably. This article has been supported by the research project "Effects of Future Snow Conditions on Tourism and Economy in Tyrol and Styria" (CC-Snow II). CC-Snow II received financial support from the Climate and Energy Fund (grant number K10AC0K00049) and was carried out within the framework of the "ACRP" Program.

## References


Anderson, E.A., 1976. A point energy and mass balance model of a snow cover. Technical Report NWS 19. NOAA.

Beniston, M., 2005. Mountain climates and climatic change: an overview of processes focusing on the European Alps. Pure Appl. Geophys. 162, 1587–1606.

Breiling, M., Charamza, P., 1999. The impact of global warming on winter tourism and skiing: a regionalised model for Austrian snow conditions. Reg. Environ. Chang. 1, 4–14.

Chen, J., Kevorkian, V., 1971. Heat and mass transfer in making artificial snow. Ind. Eng. Chem. Process Des. Dev. 10, 75–78.

Corripio, J., 2003. Vectorial algebra algorithms for calculating terrain parameters from DEMs and solar radiation modelling in mountainous terrain. Int. J. Geogr. Inf. Sci. 17, 1–23.

Dadic, R., Mott, R., Lehning, M., Burlando, P., 2010. Parameterization for wind-induced preferential deposition of snow. Hydrol. Process. 24, 1994–2006.

Dawson, J., Scott, D., 2012. Managing for climate change in the alpine ski sector. Tour. Manag. 35, 244–254.

Dozier, J., Painter, T.H., 2004. Multispectral and hyperspectral remote sensing of alpine snow properties. Annu. Rev. Earth Planet. Sci. 32, 465–494.

Eisel, L., Mills, K., Leaf, C., 1988. Estimated consumptive loss from man-made snow. JAWRA 24, 815–820.

Elsasser, H., Bürki, R., 2002. Climate change as a threat to tourism in the Alps. Clim. Res. 20, 253–257.

Elsasser, H., Messerli, P., 2001. The vulnerability of the snow industry in the Swiss Alps. Mt. Res. Dev. 21, 335–339.

Fauve, M., Rhyner, H., Schneebeli, M., 2002. Preparation and Maintenance of Pistes: Handbook for Practitioners. Swiss Federal Institute for Snow and Avalanche Research SLF.

Föhn, P., Meister, R., 1983. Distribution of snow drifts on ridge slopes: measurements and theoretical approximations. Ann. Glaciol. 4, 52–57.

Frei, C., Schär, C., 1998. A precipitation climatology of the Alps from high-resolution rain-gauge observations. Int. J. Climatol. 18, 873–900.

Fukushima, T., Kureha, M., Ozaki, N., Fujimori, Y., Harasawa, H., 2002. Influences of air temperature change on leisure industries — case study on ski activities. Mitig. Adapt. Strateg. Glob. Chang. 7, 173–189.

Goodison, B.E., Louie, P., Yang, D., 1998. WMO solid precipitation measurement intercomparison. Technical Report WMO/TD 872. World Meteorological Organization, Geneva.

Greuell, W., Knap, W.H., Smeets, P.C., 1997. Elevational changes in meteorological variables along a midlatitude glacier during summer. J. Geophys. Res. 102, 25941–25954.

Hall, D.K., Riggs, G.A., Salomonson, V.V., 1995. Development of methods for mapping global snow cover using moderate resolution imaging spectroradiometer data. Remote Sens. Environ. 54, 127–140.

Hanzer, F., 2013. Explicit Modeling of Technical Snow Production. (Master's thesis) University of Graz, Graz.

Hendrikx, J., Hreinsson, E.Ö., 2012. The potential impact of climate change on seasonal snow in New Zealand: part II — industry vulnerability and future snowmaking potential. Theor. Appl. Climatol. 110, 619–630.

Hennessy, K.J., Whetton, P.H., Smith, I.N., Bathols, J.M., Hutchinson, M., Sharples, J., 2003. The impact of climate change on snow conditions in mainland Australia. Technical Report. CSIRO Atmospheric Research Aspendale, Australia.

Hennessy, K.J., Whetton, P.H., Walsh, K., Smith, I.N., Bathols, J.M., Hutchinson, M., Sharples, J., 2008. Climate change effects on snow conditions in mainland Australia and adaptation at ski resorts through snowmaking. Clim. Res. 35, 255–270.

Jordan, R., 1991. A one-dimensional temperature model for a snow cover: technical documentation for SNTHERM. 89. Technical Report. U.S. Army Cold Regions Research and Engineering Laboratory, Hanover, NH.

Keller, T., Pielmeier, C., Rixen, C., Gadient, F., Gustafsson, D., Stahli, M., 2004. Impact of artificial snow and ski-slope grooming on snowpack properties and soil thermal regime in a sub-alpine ski area. Ann. Glaciol. 38, 314–318.

Koenig, U., Abegg, B., 1997. Impacts of climate change on winter tourism in the Swiss Alps. J. Sustain. Tour. 5, 46–58.

Liston, G.E., Elder, K., 2006. A meteorological distribution system for high-resolution terrestrial modeling (MicroMet). J. Hydrometeorol. 7, 217–234.

Luterbacher, J., Liniger, M.A., Menzel, A., Estrella, N., Della-Marta, P.M., Pfister, C., Xoplaki, E., 2007. Exceptional European warmth of autumn 2006 and winter 2007: historical context, the underlying dynamics, and its phenological impacts. Geophys. Res. Lett. 34, L12704.

Marke, T., 2008. Development and Application of a Model Interface to Couple Land Surface Models with Regional Climate Models for Climate Change Risk Assessment. (Ph.D. thesis) Ludwig-Maximilians-Universität München.

Mayer, M., Steiger, R., Trawöger, L., 2007. Technischer Schnee rieselt vom touristischen Machbarkeitshimmel. Mitt. Österr. Geogr. Ges. 149, 157–180.

Moen, J., Fredman, P., 2007. Effects of climate change on alpine skiing in Sweden. J. Sustain. Tour. 15, 418–437.

Nešpor, V., Sevruk, B., 1999. Estimation of wind-induced error of rainfall gauge measurements using a numerical simulation. J. Atmos. Ocean. Technol. 16, 450–464.

Olefs, M., Fischer, A., Lang, J., 2010. Boundary conditions for artificial snow production in the Austrian Alps. J. Appl. Meteorol. Climatol. 49, 1096–1113.

Pellicciotti, F., Brock, B., Strasser, U., Burlando, P., Funk, M., Corripio, J., 2005. An enhanced temperature-index glacier melt model including the shortwave radiation balance: development and testing for Haut Glacier d'Arolla, Switzerland. J. Glaciol. 51, 573–587.

Pickering, C.M., Buckley, R.C., 2010. Climate response by the ski industry: the shortcomings of snowmaking for Australian resorts. Ambio 39, 430–438.

Pröbstl, U., 2006. Kunstschnee und Umwelt. Entwicklung und Auswirkungen der technischen Beschneiung, Haupt, Bern, Switzerland.

Pröbstl, U., Prutsch, A., 2008. Endbericht STRATEGE. Technical Report.

Rixen, C., Teich, M., Lardelli, C., Gallati, D., Pohl, M., Puetz, M., Bebi, P., 2011. Winter tourism and climate change in the Alps: an assessment of resource consumption, snow reliability, and future snowmaking potential. Mt. Res. Dev. 31, 229–236.

Rohrer, M.B., 1992. Die Schneedecke im schweizerischen Alpenraum und ihre Modellierung. Zür. Geogr. Schrift. 49.

Schirmer, M., Wirz, V., Clifton, A., Lehning, M., 2011. Persistence in intra-annual snow depth distribution: 1. Measurements and topographic control. Water Resour. Res. 47, W09516.

Schmidt, R.A., Troendle, C.A., 1989. Snowfall into a forest and clearing. J. Hydrol. 110, 335–348.

Schmidt, P., Steiger, R., Matzarakis, A., 2012. Artificial snowmaking possibilities and climate change based on regional climate modeling in the Southern Black Forest. Meteorol. Z. 21, 167–172.

Scott, D., McBoyle, G., 2007. Climate change adaptation in the ski industry. Mitig. Adapt. Strateg. Glob. Chang. 12, 1411–1431.

Scott, D., McBoyle, G., Mills, B., 2003. Climate change and the skiing industry in southern Ontario (Canada): exploring the importance of snowmaking as a technical adaptation. Clim. Res. 23, 171–181.

Scott, D., McBoyle, G., Minogue, A., Mills, B., 2006. Climate change and the sustainability of ski-based tourism in eastern North America: a reassessment. J. Sustain. Tour. 14, 376–398.

Scott, D., McBoyle, G., Minogue, A., 2007. Climate change and Quebec's ski industry. Glob. Environ. Chang. 17, 181–190.

Steiger, R., 2010. The impact of climate change on ski season length and snowmaking requirements in Tyrol, Austria. Clim. Res. 43, 251–262.

Steiger, R., 2011. The impact of snow scarcity on ski tourism: an analysis of the record warm season 2006/2007 in Tyrol (Austria). Tour. Rev. 66, 4–13.

Steiger, R., Mayer, M., 2008. Snowmaking and climate change. Mt. Res. Dev. 28, 292–298.

Strasser, U., 2004. Spatial and temporal variability of meteorological variables at Haut Glacier d'Arolla (Switzerland) during the ablation season 2001: measurements and simulations. J. Geophys. Res. 109, D03103.

Strasser, U., 2008. Modelling of the mountain snow cover in the Berchtesgaden National Park. Technical Report 55. Berchtesgaden National Park, Berchtesgaden.

Strasser, U., Bernhardt, M., Weber, M., Liston, G.E., Mauser, W., 2008. Is snow sublimation important in the alpine water balance? Cryosphere 2, 53–66.

Varhola, A., Coops, N.C., Weiler, M., Moore, R.D., 2010. Forest canopy effects on snow accumulation and ablation: an integrative review of empirical results. J. Hydrol. 392, 219–233.